Emergent SO(5) symmetry in the global phase diagram of extended Hubbard model in monolayer graphene

Bitan Roy

Lehigh University, Bethlehem, PA

A. Szabo & **BR** *To appear on arXiv*

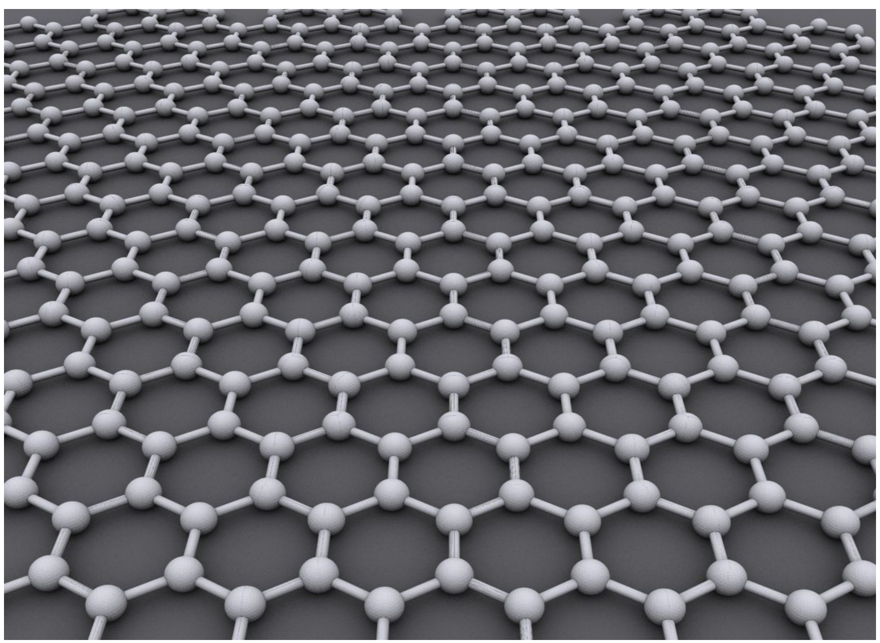

Relativistic Fermions in Flatland: Theory and Application, 2021

Symmetries

Exact

Emergent

- Exact symmetry → Time reversal, SU(2) spin rotational symmetry
- Emergent symmetry → Lorentz symmetry, Chiral symmetry, ...

PRB **79**, 085116 (2009), JHEP **04**, 018 (2016)

High energy or UV

Isospin doublet: electron & electron neutrino
Unification of electromagnetic &
weak forces SU(2) x U(1) symmetry (>246 GeV)

Nucl. Phys. **10**, 107 (1959); Nuovo Cimento **11**, 568 (1959);
PRL **19**, 1264 (1967)

Low energy or IR

Topological phase transition in *d=3*:
Emergent U(1) chiral symmetry

PRB **94**, 041101(R) (2016)

Topological phase transition

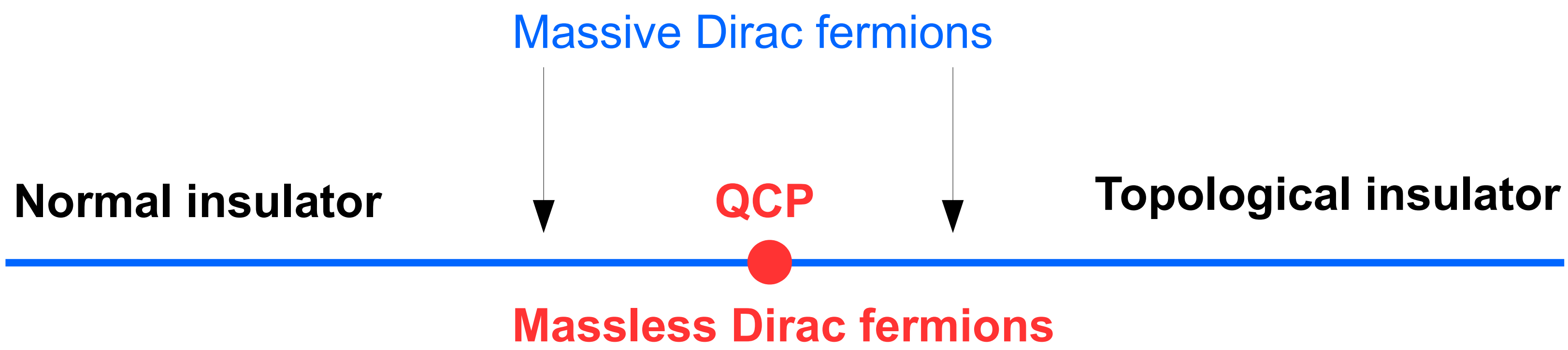

- Hamiltonian: $H = v \sum_{j=1,2,3} i\gamma_0 \gamma_j k_j + \left(m - bk^2\right)\gamma_0$

  v : Fermi velocity
  m : Regular Dirac mass
  b : Higher gradient term (>0)

  Science **314**, 1157 (2006); PRB **82**, 045122 (2010)

- Imaginary time action: $S = \int d^3x \, d\tau \, \Psi^\dagger(\tau, \boldsymbol{x}) \left[\partial_\tau + H(\boldsymbol{k} \to -i\boldsymbol{\nabla})\right] \Psi(\tau, \boldsymbol{x})$

- Phase diagram: *m > 0* : topological insulator, *m < 0* : trivial or normal insulator

  Quantum phase transition (QPT) @ *m=0*

- Symmetry under global chiral rotation: $\Psi(\tau, \boldsymbol{x}) \to e^{i\theta\gamma_5}\Psi(\tau, \boldsymbol{x}), \quad \Psi^\dagger(\tau, \boldsymbol{x}) \to \Psi^\dagger(\tau, \boldsymbol{x}) e^{-i\theta\gamma_5}$

  Broken when $m, b \neq 0$

Emergent symmetry: An example

- Topological phase transition in the renormalization group (RG) language:

$$\frac{dv}{d\ell} = 0, \quad \frac{dm}{d\ell} = m, \quad \frac{db}{d\ell} = -b$$

ℓ : Logarithm of the RG time

Determined by the bare scaling dimensions for a *z=1* or Dirac system

- Fermi velocity: *marginal*, Dirac mass: *relevant*, *b*: *irrelevant*

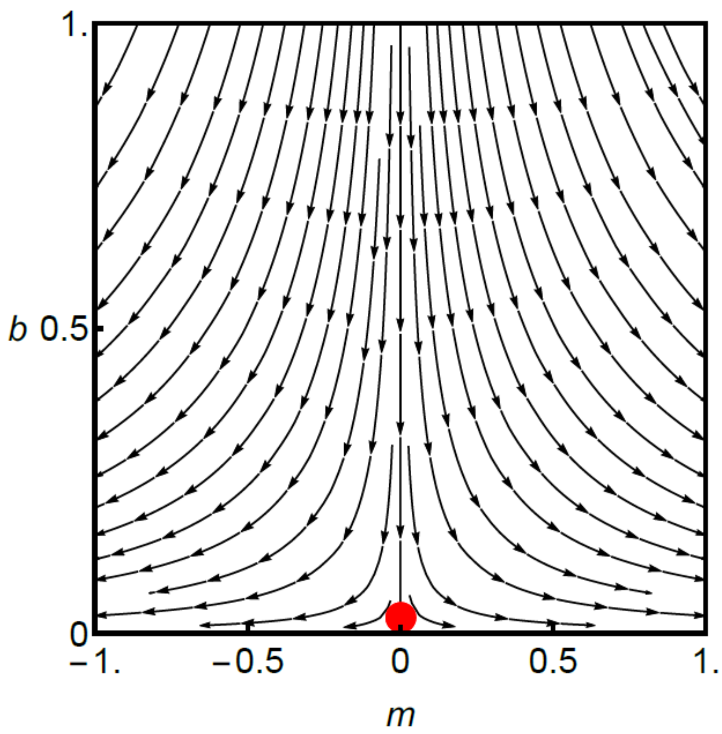

Topological quantum critical point: located @

$$(m, b) = (0, 0)$$

U(1) chiral symmetry: Absent @ microscopic level

but restored @ a scale invariant QCP

Emergent phenomena!

BR, P. Goswami & J. D. Sau, PRB **94**, 041101(R) (2016)

Emergent symmetry in correlated systems

Interacting Dirac liquid on a flatland

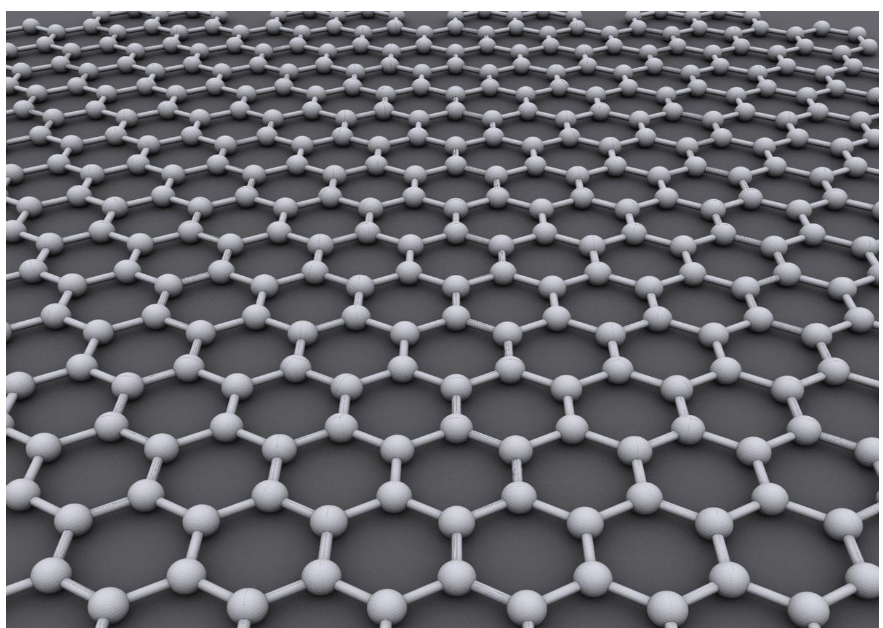

Dirac fermions in graphene

- Honeycomb lattice: Two interpenetrating triangular sublattices

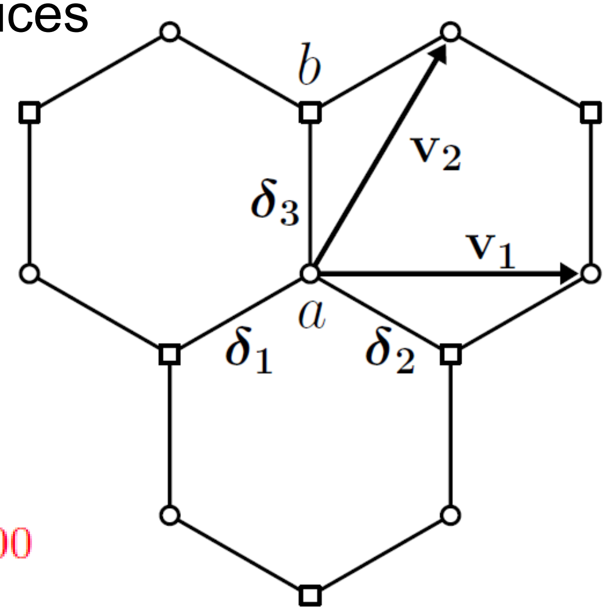

Lack of inversion symmetry about site centers
→ Fermi points @ corners of Brillouin zone

RMP **81**, 109 (2009)

- Low-energy Hamiltonian for massless Dirac fermions:

$$\hat{h}_{\mathrm{D}}(\boldsymbol{k}) = v\left[\Gamma_{3031}k_x - \Gamma_{3002}k_y\right] - \mu\Gamma_{3000}$$

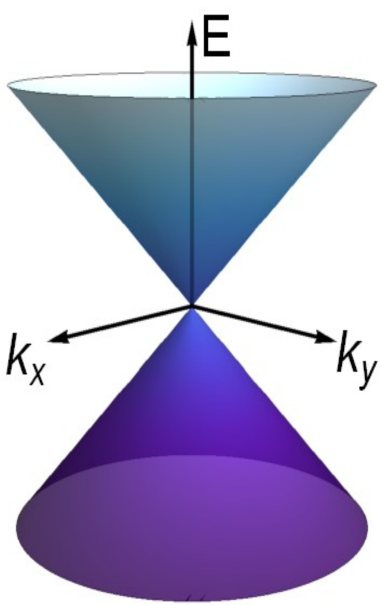

$$\Gamma_{\mu\nu\lambda\rho} = \eta_\mu \otimes \sigma_\nu \otimes \tau_\lambda \otimes \alpha_\rho \equiv \mu\nu\lambda\rho$$

$$\mu, \nu, \rho, \lambda = 0, 1, 2, 3$$

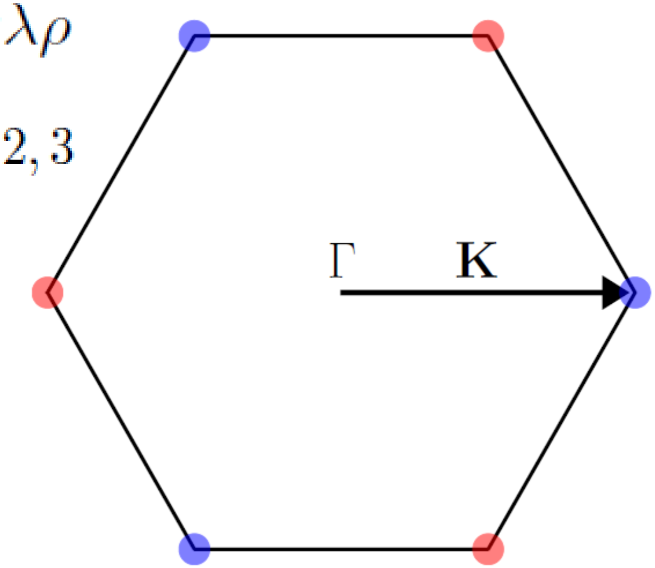

Pauli matrices

α_ρ : Sublattice $\quad$ τ_λ : Valley

σ_ν : Spin $\quad$ η_μ : Nambu

Symmetries in Dirac system

- Sublattice reflection: $S = \Gamma_{0001} \oplus \begin{pmatrix} k_x \to k_x \\ k_y \to -k_y \end{pmatrix}$

- Valley reflection: $T = \Gamma_{0010} \oplus \begin{pmatrix} k_x \to -k_x \\ k_y \to k_y \end{pmatrix}$

- Spatial Rotation: $R\left(\frac{\pi}{2}\right) = \exp\left(i\frac{\pi}{2}\Gamma_{0033}/2\right) \oplus \begin{pmatrix} k_x \to -k_y \\ k_y \to k_x \end{pmatrix}$

- Translation: U(1) rotation generated by $I_{\mathrm{tr}} = \Gamma_{0030}$

- Time reversal: Generated by *antiunitary* operator $\mathcal{T} = \Gamma_{0210}\,\mathcal{K}$

- SU(2) spin rotational symmetry: Generated by $\boldsymbol{S} = \{\Gamma_{0100}, \Gamma_{0200}, \Gamma_{0300}\}$

PRB **79**, 085116 (2009), PRB **103**, 205135 (2021)

Interactions among Dirac fermions

Long range Coulomb interaction

Short range Hubbardlike interaction

Marginally irrelevant → Renormalization of Fermi velocity
→ logarithmic enhancement of Fermi velocity → Experimentally observed
: Remains unchanged even for strong enough bare Coulomb coupling

PRB **59**, R2474 (1999); PRL **97**, 146401 (2006); PRB **75**, 235423 (2007);
PRB **80**, 081405(R) (2009); PRB **87**, 045425 (2013); PRL **113**, 105502 (2013)

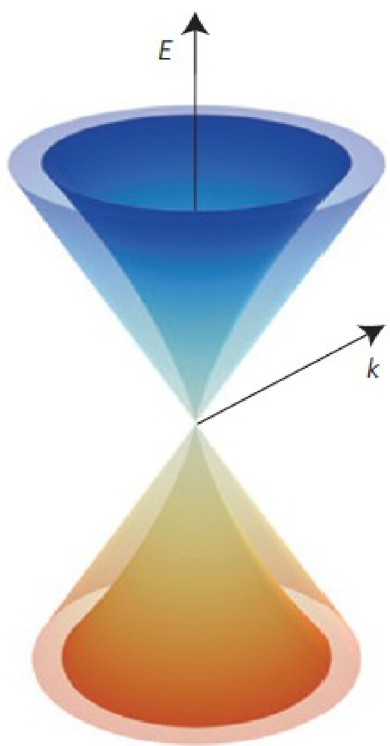

No instability of Dirac liquid by pure long range Coulomb interaction!
PRL **118**, 026403 (2017)

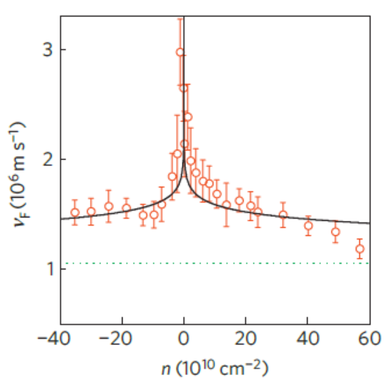

Nat. Phys. **7**, 701 (2011)

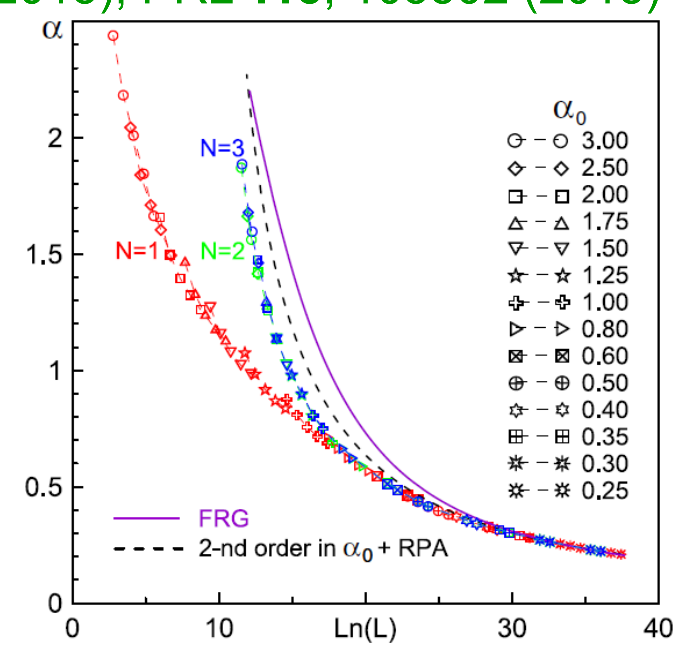

Hubbardlike interactions

- Weak short-range interactions: *irrelevant* → Stable Dirac liquid
- Sufficiently strong short-range interactions: *relevant*
  → spontaneous symmetry breaking → onset of ordered states
- At T=0: Best candidates for ordered states → *dynamic generation of Dirac mass*

Through quantum phase transitions via **quantum critical points (QCPs)**

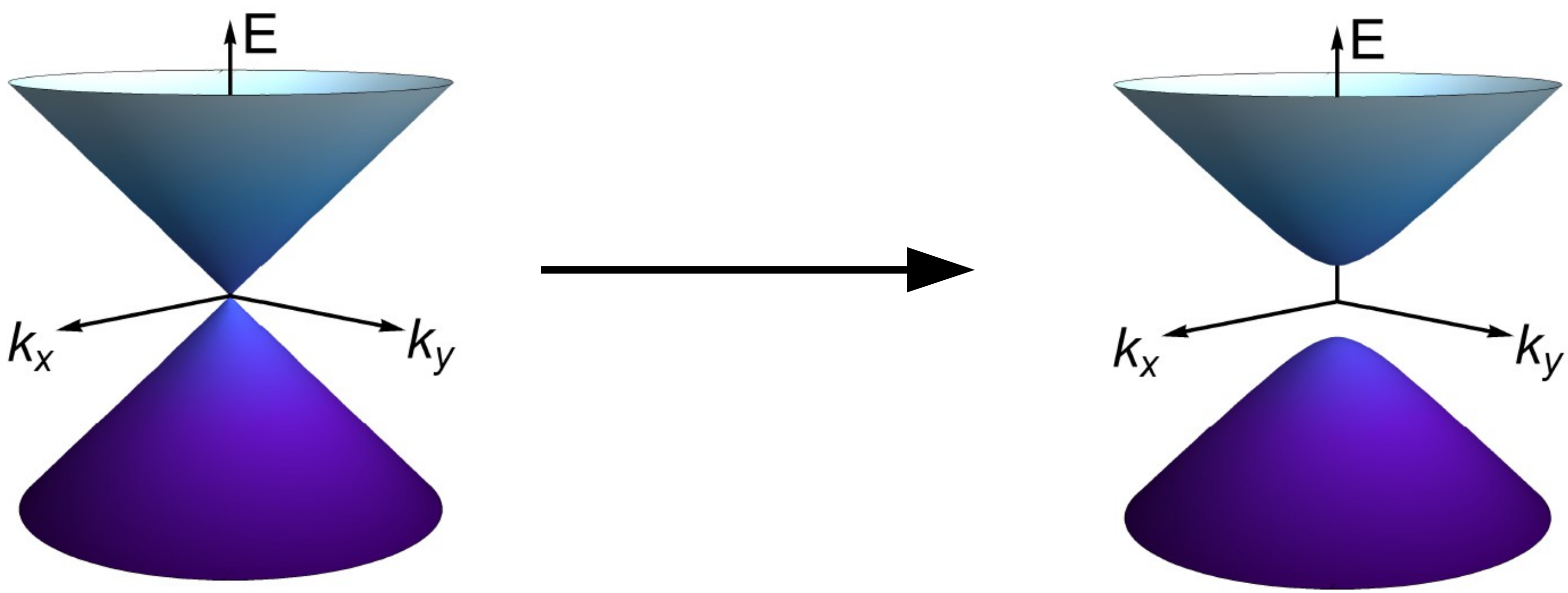

Spontaneous breaking of discrete (crystal or fundamental) and/or continuous symmetry

6 excitonic & 3 superconducting masses

Dirac masses: singlet excitonic

- Charge density wave (CDW):
  Breaks sublattice symmetry

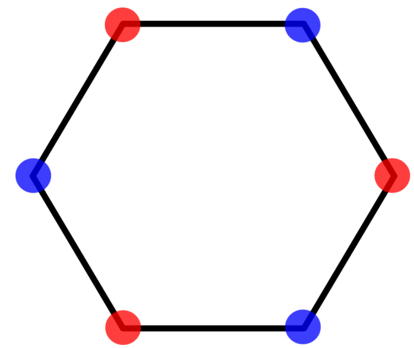

$$\Gamma_{3003}$$

Semenoff PRL **53**, 2449 (1983)

- Quantum anomalous Hall insulator (QAHI):
  Breaks sublattice & time reversal symmetries

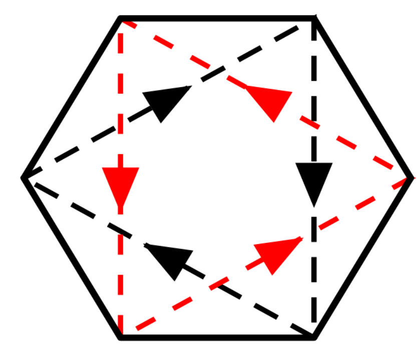

$$\Gamma_{0033}$$

Haldane PRL **61**, 2015 (1988)

- Kekule valence bond solid (KVBS):
  Breaks translational symmetry

$$(\Gamma_{3011}, \Gamma_{3021})$$

Hou, Chamon, Mudry
PRL **98**, 186809 (2007)

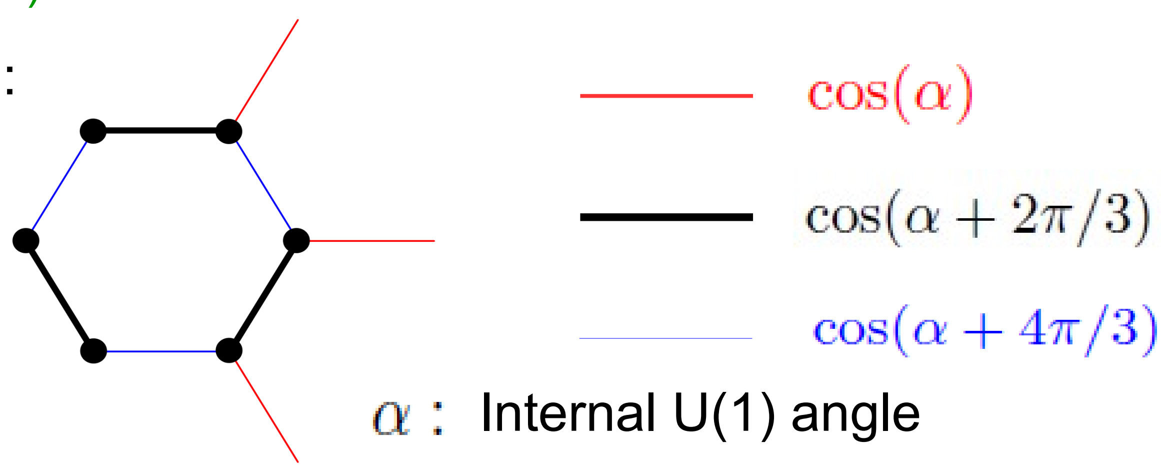

Dirac masses: Triplet excitonic

- Antiferromagnet (AFM): Breaks sublattice & spin rotational symmetries

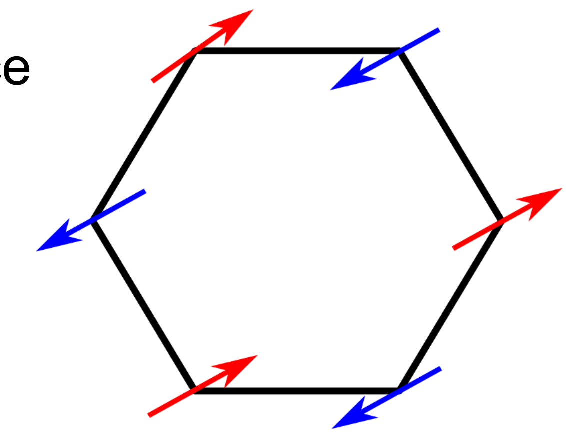

$$(\Gamma_{0103}, \Gamma_{0203}, \Gamma_{0303})$$

Herbut PRL **97**, 085116 (2006)

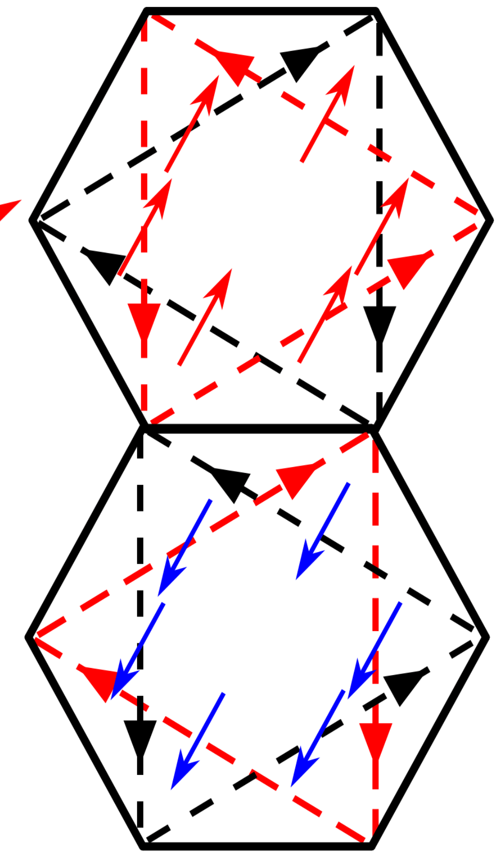

- Quantum spin Hall insulator (QSHI): Breaks sublattice & spin rotational symmetries

$$(\Gamma_{3133}, \Gamma_{3233}, \Gamma_{3333})$$

Raghu, Qi, Honerkamp & Zhang PRL **100**, 156401 (2008)

- Spin Kekule valence bond solid (SKVBS): Breaks translational & spin rotational symmetries

$$(\Gamma_{0j11}, \Gamma_{0j21}) \quad j = 1, 2, 3$$

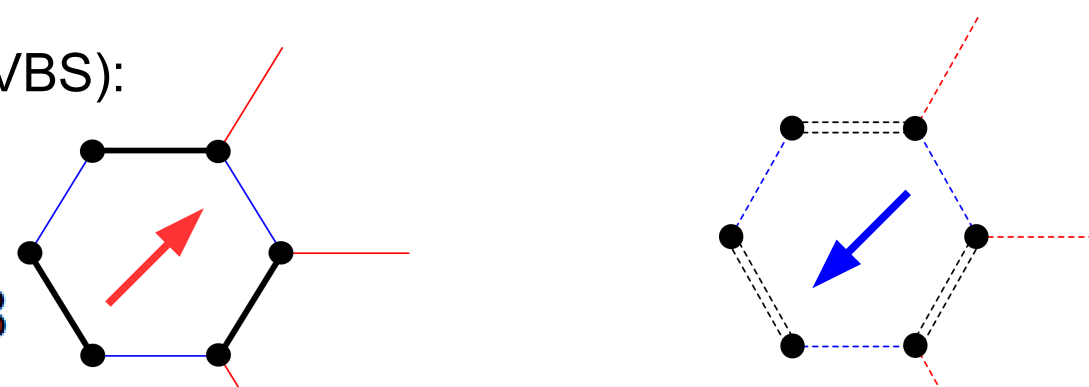

Roy & Herbut PRB **93**, 155415 (2016)

Dashed lines = - Solid lines

Dirac masses: Superconducting

- *s*-wave pairing (singlet):
  Breaks global U(1) symmetry

$$(\Gamma_{1000}, \Gamma_{2000})$$

Zhao & Paramekanti PRL **97**, 230404 (2006)

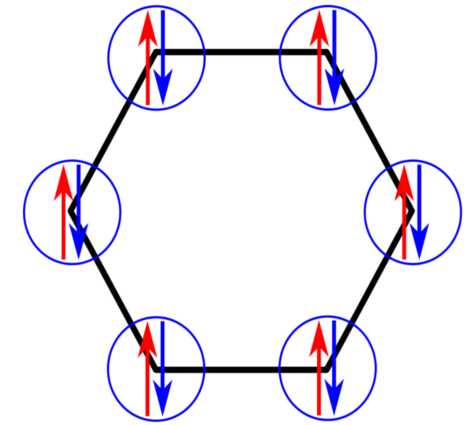

- *f*-wave pairing (triplet):
  Breaks valley & spin
  rotational symmetries

$$(\Gamma_{1j30}, \Gamma_{2j30}) \quad j = 1, 2, 3$$

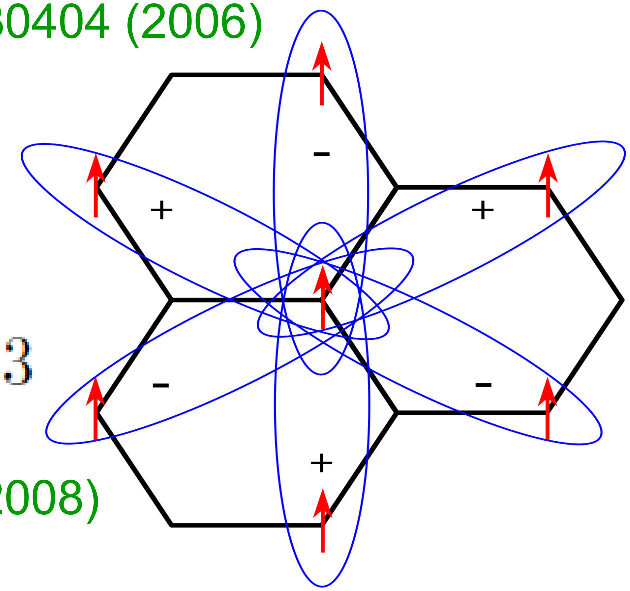

Honerkamp PRL **100**, 146404 (2008)

- Kekule superconductor (triplet):
  Breaks translational & spin
  rotational symmetries

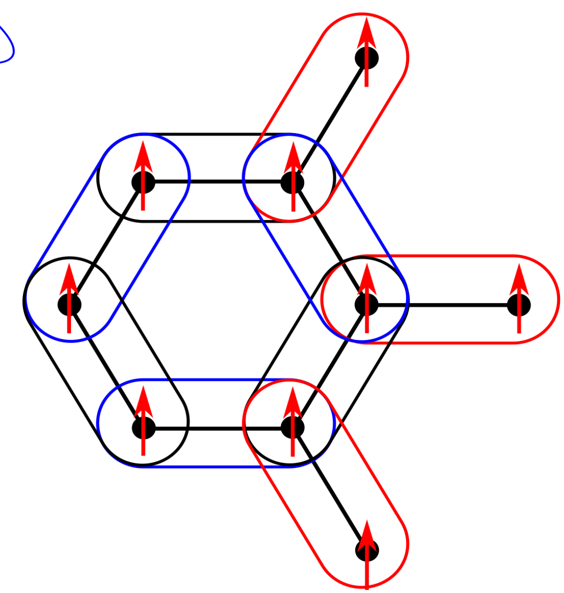

$$(\Gamma_{\alpha j12}, \Gamma_{\alpha j22}) \quad j = 1, 2, 3 \quad \alpha = 1, 2$$

Roy & Herbut PRB **82**, 035429 (2010)

Competing Dirac masses

- Antiferromagnet & Kekule valence bond solid: SO(5) symmetry

  (0103,0203,0303): Antiferromagnet
  (3011,3021): Kekule valence bond solid

  (0100,0200,0300): SU(2) Spin rotation
  0030: Generator of translation
  Remaining 6: General chiral rotations

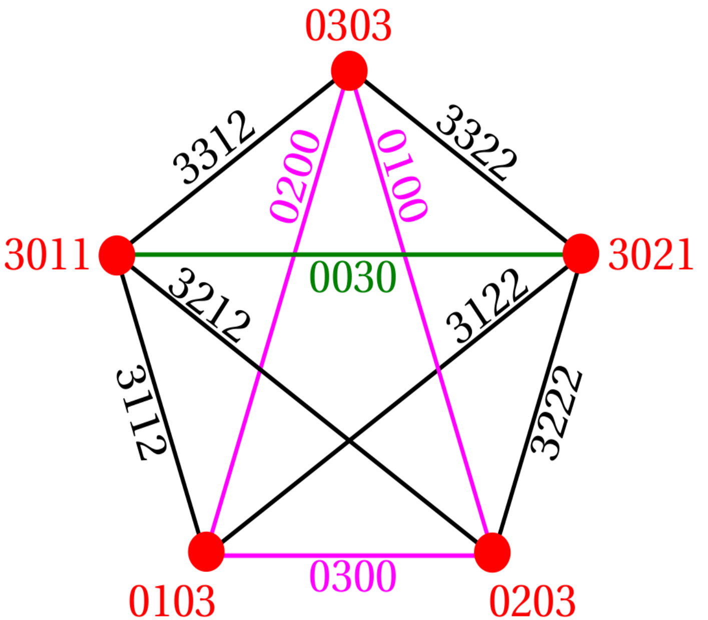

- Quantum spin Hall insulator & *s*-wave pairing: SO(5) symmetry

  (3133,3233,3333): Quantum spin Hall insulator
  (1000,2000): *s*-wave pairing

  (0100,0200,0300): SU(2) Spin rotation
  3000: Number operator
  Remaining 6: General chiral rotations

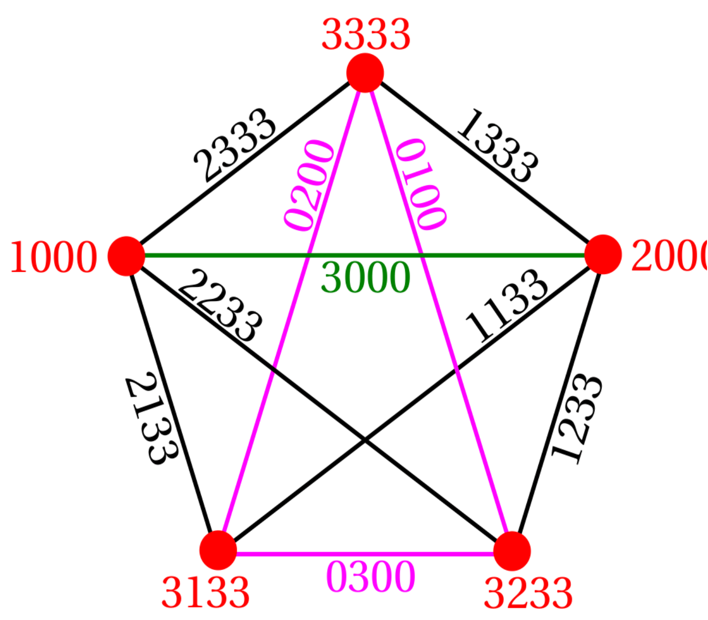

Competing Dirac masses

- Charge-density-wave, Kekule valence bond solid & *s*-wave pairing: SO(5) symmetry

  3003: Charge-density-wave
  (3011,3021): Kekule valence bond solid
  (1000,2000): *s*-wave pairing

  (1003,2003,3000): SU(2) pseudo-spin rotation
  0030: Generator of translation
  Remaining 6: General chiral rotations

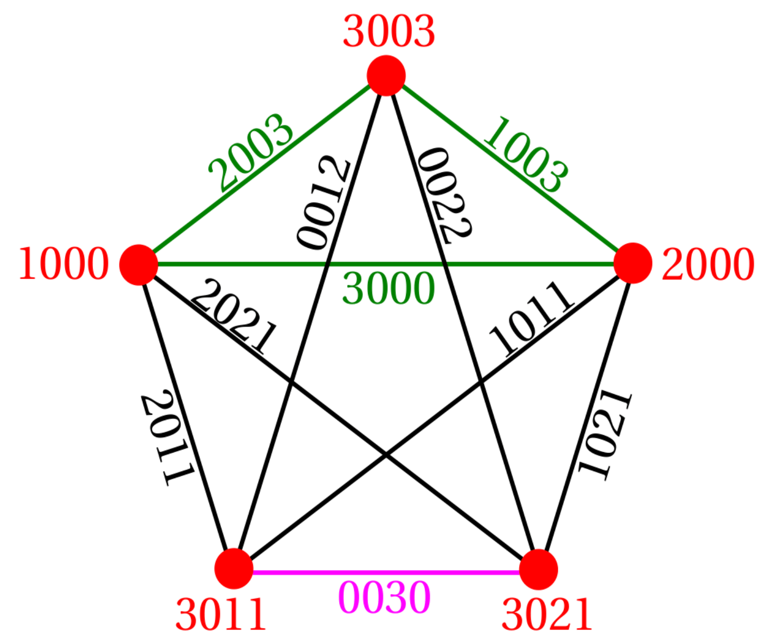

Largest symmetry among competing Dirac masses in graphene: SO(5)
Only **3** such candidates consistent with microscopic symmetries

Five tuplet	Partner five-tuplet by C conjugation
{Re VBS, Im VBS, Re SSC, Im SSC, CDW}	{Re VBS, Im VBS, Néel$_x$, Néel$_y$, Néel$_z$}
{Im VBS, CDW, Re VBS$_x$, Re VBS$_y$, Re VBS$_z$}	{Im VBS, Néel$_z$, Im TSC$_{32z}$, Re TSC$_{32z}$, Re VBS$_z$}
{Re VBS, CDW, Im VBS$_x$, Im VBS$_y$, Im VBS$_z$}	{Re VBS, Néel$_z$, Re TSC$_{02z}$, Im TSC$_{02z}$, Im VBS$_z$}
{Re SSC, Im SSC, QSHE$_x$, QSHE$_y$, QSHE$_z$}	{Néel$_x$, Néel$_y$, Im TSC$_z$, Re TSC$_z$, QSHE$_z$}
{Re VBS, Re SSC, Re TSC$_{02x}$, Im TSC$_{02y}$, Re TSC$_{02z}$}	{Re VBS, Néel$_x$, Re TSC$_{02x}$, Im TSC$_{02x}$, Im VBS$_x$}
{Re VBS, Im SSC, Im TSC$_{02x}$, Re TSC$_{02y}$, Im TSC$_{02z}$}	{Re VBS, Néel$_y$, Im TSC$_{02y}$, Re TSC$_{02y}$, Im VBS$_y$}
{Im VBS, Im SSC, Re TSC$_{32x}$, Im TSC$_{32y}$, Re TSC$_{32z}$}	{Im VBS, Néel$_y$, Re TSC$_{32y}$, Im TSC$_{32y}$, Re VBS$_y$}
{Im VBS, Re SSC, Im TSC$_{32x}$, Re TSC$_{32y}$, Im TSC$_{32z}$}	{Im VBS, Néel$_x$, Im TSC$_{32x}$, Re TSC$_{32x}$, Re VBS$_x$}
{CDW, Im SSC, Im TSC$_x$, Re TSC$_y$, Im TSC$_z$}	{Néel$_z$, Néel$_y$, Im TSC$_x$, Re TSC$_x$, QSHE$_x$}
{CDW, Re SSC, Re TSC$_x$, Im TSC$_y$, Re TSC$_z$}	{Néel$_z$, Néel$_x$, Re TSC$_y$, Im TSC$_y$, QSHE$_y$}
{Im VBS$_x$, QSHE$_y$, Im VBS$_z$, Re TSC$_{32y}$, Im TSC$_{32y}$}	{Re TSC$_{02z}$, Re TSC$_z$, Im VBS$_z$, Re TSC$_{32x}$, Im TSC$_{32y}$}
{Im VBS$_x$, QSHE$_y$, Re VBS$_x$, Néel$_x$, QSHE$_z$}	{Re TSC$_{02z}$, Re TSC$_z$, Im TSC$_{32z}$, Re SSC, QSHE$_z$}
{Im VBS$_x$, Re TSC$_{32y}$, Im TSC$_{32z}$, Im TSC$_{02x}$, Im TSC$_x$}	{Re TSC$_{02z}$, Re TSC$_{32x}$, Re VBS$_x$, Im TSC$_{02y}$, Im TSC$_x$}
{Im VBS$_x$, Re TSC$_{32z}$, Re TSC$_{02x}$, Re TSC$_x$, Im TSC$_{32y}$}	{Re TSC$_{02z}$, Re VBS$_y$, Re TSC$_{02x}$, Re TSC$_y$, Im TSC$_{32y}$}
{Im VBS$_x$, Re TSC$_{32z}$, Im TSC$_{32z}$, Im VBS$_y$, QSHE$_z$}	{Re TSC$_{02z}$, Re VBS$_y$, Re VBS$_x$, Im TSC$_{02z}$, QSHE$_z$}
{Im VBS$_x$, Re TSC$_x$, Im TSC$_x$, CDW, Re VBS$_x$}	{Re TSC$_{02z}$, Re TSC$_y$, Im TSC$_x$, Néel$_z$, Im TSC$_{32z}$}
{QSHE$_y$, Im VBS$_z$, QSHE$_x$, Re VBS$_z$, Néel$_z$}	{Re TSC$_z$, Im VBS$_z$, Im TSC$_z$, Re VBS$_z$, CDW}
{QSHE$_y$, Re TSC$_{02y}$, Re TSC$_y$, Im SSC, Im TSC$_{32y}$}	{Re TSC$_z$, Re TSC$_{02y}$, Re TSC$_x$, Néel$_y$, Im TSC$_{32y}$}
{QSHE$_y$, Re TSC$_{02y}$, Im TSC$_{02y}$, Re VBS$_x$, Re VBS$_z$}	{Re TSC$_z$, Re TSC$_{02y}$, Im TSC$_{02x}$, Im TSC$_{32z}$, Re VBS$_z$}
{QSHE$_y$, Re TSC$_{32y}$, Im TSC$_{02y}$, Im TSC$_y$, Re SSC}	{Re TSC$_z$, Re TSC$_{32x}$, Im TSC$_{02x}$, Im TSC$_y$, Néel$_x$}
{Re VBS$_y$, Néel$_y$, QSHE$_x$, Im VBS$_y$, QSHE$_z$}	{Re TSC$_{32z}$, Im SSC, Im TSC$_z$, Im TSC$_{02z}$, QSHE$_z$}
{Re VBS$_y$, Re TSC$_y$, Im TSC$_y$, CDW, Im VBS$_y$}	{Re TSC$_{32z}$, Re TSC$_x$, Im TSC$_y$, Néel$_z$, Im TSC$_{02z}$}
{Re VBS$_y$, Re TSC$_{32y}$, Im TSC$_y$, Im TSC$_{02z}$, Im TSC$_{02x}$}	{Re TSC$_{32z}$, Re TSC$_{32x}$, Im TSC$_y$, Im VBS$_y$, Im TSC$_{02y}$}
{Re VBS$_y$, Re TSC$_{02x}$, Im TSC$_{02x}$, QSHE$_x$, Re VBS$_z$}	{Re TSC$_{32z}$, Re TSC$_{02x}$, Im TSC$_{02y}$, Im TSC$_z$, Re VBS$_z$}
{Néel$_y$, Re TSC$_{32y}$, Im TSC$_{02y}$, Im TSC$_z$, Im TSC$_x$}	{Im SSC, Re TSC$_{32x}$, Im TSC$_{02x}$, QSHE$_x$, Im TSC$_x$}
{Im VBS$_z$, Re TSC$_{32y}$, Im TSC$_{02z}$, Im TSC$_z$, Im TSC$_{32x}$}	{Im VBS$_z$, Re TSC$_{32x}$, Im VBS$_y$, QSHE$_x$, Im TSC$_{32x}$}
{Re TSC$_{02y}$, Re TSC$_y$, Im TSC$_{32z}$, Im TSC$_{32x}$, Im VBS$_y$}	{Re TSC$_{02y}$, Re TSC$_x$, Re VBS$_x$, Im TSC$_{32x}$, Im TSC$_{02z}$}
{Re TSC$_y$, Re TSC$_{02x}$, Im TSC$_z$, Im TSC$_{32x}$, Néel$_x$}	{Re TSC$_x$, Re TSC$_{02x}$, QSHE$_x$, Im TSC$_{32x}$, Re SSC}

Ryu, Mudry, Hou, Chamon PRB **80**, 205319 (2009)

Internal symmetry among competing orders → emergent symmetry @ QCPs?

Setup

- Begin with generic four-fermion interactions:

$$g_{MN}\left(\Psi^\dagger M \Psi\right)\left(\Psi^\dagger N \Psi\right)$$

g_{MN}: Coupling constant, *M* & *N* matrices operating on *sublattice, valley & spin indices*

- Impose discrete and continuous microscopic symmetries
→ Number of coupling constants **544 → 18**

- Fierz relation:

$$[\Psi^\dagger(x) M \Psi(x)][\Psi^\dagger(y) N \Psi(y)]$$
$$= -\frac{1}{64}\mathrm{Tr}(M\Gamma^a N \Gamma^b)[\Psi^\dagger(x)\Gamma^b\Psi(y)][\Psi^\dagger(y)\Gamma^a\Psi(x)]$$

Herbut, Juricic & BR PRB **79**, 085116 (2009); O. Vafek PRB **82**, 205106 (2010)

Number of linearly independent coupling constants = 18 – 9 = 9 for *x* = *y*

Results are insensitive to the choices of 9 couplings!

Scaling analysis

- Euclidean action in the presence of *e-e* interactions: $S_{\text{total}} = S_0 + S_{\text{int}}$

$$S_0 = \int d\tau \int d^d x\, \Psi^\dagger(\tau, x) \left[\partial_\tau + \hat{h}_{\mathrm{D}}(k \to -i\boldsymbol{\nabla})\right] \Psi(\tau, x)$$

$$S_{\text{int}} = g_M \int d\tau \int d^d x \left[\Psi^\dagger(\tau, x) M \Psi(\tau, x)\right]^2$$

- Scaling dimension: $[g_M] = d - z = 2 - 1 = -1$ → Weak interactions: irrelevant

To capture intermediate & strong coupling phenomena $d \to 1 + \epsilon$

$$[g_M] = -\epsilon$$

Controlled perturbative expansion about lower-critical one spatial dimension *(d=1)*

Feynman diagrams

Feynman diagrams & RG flow

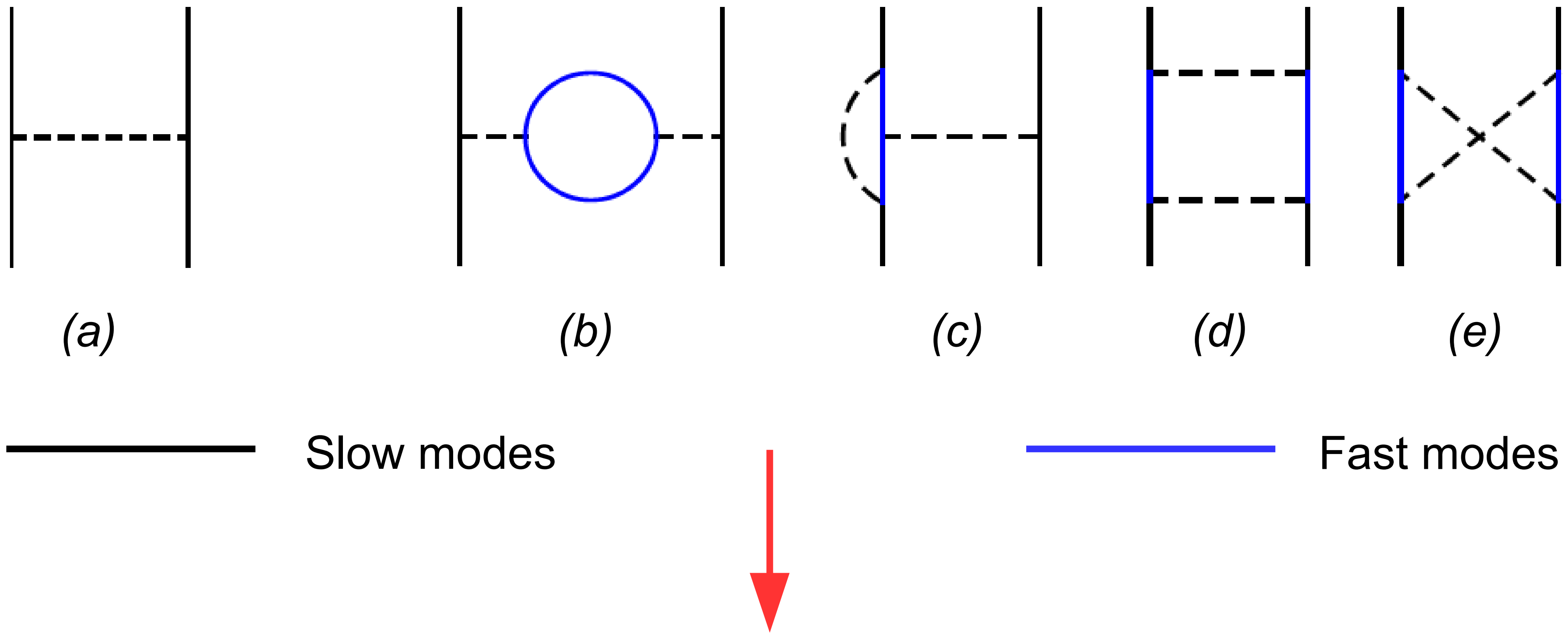

Renormalization group flow equations

$$\frac{dg_i}{d\ell} = -\epsilon g_i + \sum_{j,k=1}^{9} H_i^{jk} g_j g_k \qquad i = 1, \cdots, 9$$

Matrix algebra is performed in *d*=2 & shell integration in $d = 1 + \epsilon$

RG fixed points

- Fixed points: obtained from the zeros of the coupled RG flow equations

$$\frac{dg_i}{d\ell} = 0, \quad i = 1, \cdots, 9$$

- Fully stable Gaussian fixed points → stable DSM phase (weak interactions)

$$\{g_i\} \equiv 0$$

- Infrared unstable (in one direction) QCPs → Continuous QPTs to various ordered phases: **5**

$$\{g_i\} \sim \epsilon$$

- Unstable (in two directions) bi-critical points → Typically separates basins of attraction of different QCPs: **9**

$$\{g_i\} \sim \epsilon$$

QCP	Coupling constants (in units of ϵ)								
	$g^s_{A_{1g}}$	$g^s_{A_{2g}}$	$g^s_{A_{2u}}$	$g^s_{A_{1\mathbf{k}}}$	$g^s_{A_{1u}}$	$g^t_{A_{1g}}$	$g^t_{A_{2g}}$	$g^t_{A_{2u}}$	$g^s_{A_{1\mathbf{k}}}$
QCP_1	0.00	0.67	0.00	0.00	0.00	0.00	0.00	0.00	0.00
QCP_2	0.00	0.00	0.67	0.00	0.00	0.00	0.00	0.00	0.00
QCP_3	-0.09	-0.12	0.10	0.10	0.00	-0.04	0.38	-0.14	-0.14
QCP_4	0.00	-0.03	0.42	0.42	0.00	0.04	0.14	-0.14	-0.14
QCP_5	0.00	0.04	-0.06	0.25	-0.09	-0.04	-0.02	0.26	0.02

Symmetry analysis @ QCPs

- Couple massless Dirac excitation with all symmetry allowed fermion bilinears via conjugate field

$$S = \int d\tau \int d^d x \, \Delta_O \Psi^\dagger(\tau, x) O \Psi(\tau, x)$$

  - 9 spin-singlet particle-hole & 9 spin triplet particle-hole orders
  - 5 spin-singlet & 4 spin-triplet parings

IREP (D_{3d})	Matrix (N)	Phase
A_{1g}	Γ_{3000}	fermionic density
A_{2g}	Γ_{0033}	quantum anomalous Hall ins.
E_g	$\Gamma_{3001}, \Gamma_{3032}$	nematic$_1$
A_{1u}	Γ_{0030}	chiral density
A_{2u}	Γ_{3003}	charge-density-wave
E_u	$\Gamma_{0031}, \Gamma_{0002}$	nematic$_2$
A_{1k}	$\Gamma_{3011}, \Gamma_{3021}$	Kekulé valence bond solid
A_{2k}	$\Gamma_{0012}, \Gamma_{0022}$	Kekulé current
E_k	$\Gamma_{3010}, \Gamma_{3023}$ $\Gamma_{3013}, \Gamma_{3020}$	smectic charge-density-wave

PRB **103**, 205135 (2021)

A_{1g}	Γ_{0s00}	ferromagnet
A_{2g}	Γ_{3s33}	quantum spin Hall ins.
E_g	$\Gamma_{0s01}, \Gamma_{0s32}$	spin-nematic$_1$
A_{1u}	Γ_{3s30}	chiral ferromagnet
A_{2u}	Γ_{0s03}	antiferromagnet
E_u	$\Gamma_{3s31}, \Gamma_{3s02}$	spin-nematic$_2$
A_{1k}	$\Gamma_{0s11}, \Gamma_{0s21}$	spin-Kekulé solid
A_{2k}	$\Gamma_{3s12}, \Gamma_{3s22}$	spin-Kekulé current
E_k	$\Gamma_{0s10}, \Gamma_{0s23}$ $\Gamma_{0s13}, \Gamma_{0s20}$	smectic spin-density-wave

IREP (D_{3d})	Matrix (N)	Phase
A_{1g}	$\Gamma_{\alpha 000}$	s-wave SC
A_{2g}	$\Gamma_{\alpha s33}$	fully gapless SC$_1$
E_g	$\Gamma_{\alpha 001}, \Gamma_{\alpha 032}$	nematic SC$_1$
A_{1u}	$\Gamma_{\alpha s30}$	f-wave SC
A_{2u}	$\Gamma_{\alpha 003}$	fully gapless SC$_2$
E_u	$\Gamma_{\alpha s31}, \Gamma_{\alpha s02}$	nematic SC$_2$
A_{1k}	$\Gamma_{\alpha 011}, \Gamma_{\alpha 021}$	singlet Kekulé SC
A_{2k}	$\Gamma_{\alpha s12}, \Gamma_{\alpha s22}$	triplet Kekulé SC
E_k	$\Gamma_{\alpha 010}, \Gamma_{\alpha 023}$ $\Gamma_{\alpha 013}, \Gamma_{\alpha 020}$	smectic SC

Symmetry analysis @ QCPs

- Compute the RG flow equations for the conjugate fields:

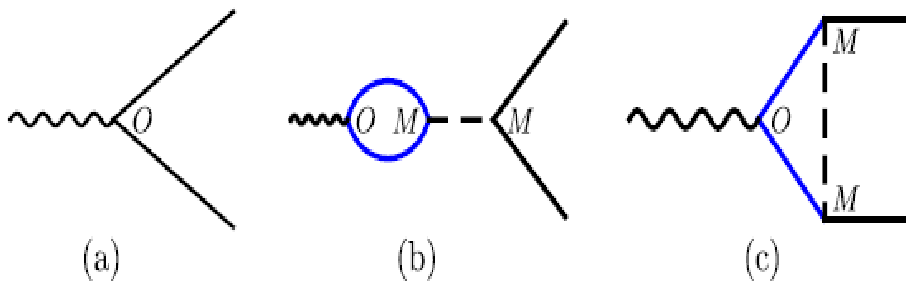

$$\frac{d \ln \Delta_O}{d\ell} - z = \sum_{j=1}^{9} S_O^j \, g_j$$

RHS of the flow equation → scaling dimension of order parameter

@ fixed points when $\{g_i\} \equiv \{g_i^\star\}$

QCP	Scaling dimension of fermion bilinears (in units of ϵ)																	
	Singlet particle-hole									Triplet particle-hole								
	A_{1g}	A_{2g}	E_g	A_{1u}	A_{2u}	E_u	$A_{1\mathrm{K}}$	$A_{2\mathrm{K}}$	E_{K}	A_{1g}	A_{2g}	E_g	A_{1u}	A_{2u}	E_u	$A_{1\mathrm{K}}$	$A_{2\mathrm{K}}$	E_{K}
QCP_1	0.00	1.17	0.08	0.00	-0.17	0.08	-0.17	0.00	0.08	0.00	-0.17	0.08	0.00	-0.17	0.08	-0.17	0.00	0.08
QCP_2	0.00	-0.17	0.08	0.00	1.17	0.08	0.17	0.00	-0.08	0.00	-0.17	0.08	0.00	-0.17	0.08	0.17	0.00	-0.08
QCP_3	0.00	-0.19	0.19	0.00	-0.08	0.03	-0.09	0.00	0.19	0.00	0.71	-0.09	0.00	-0.09	0.03	-0.09	0.00	-0.09
QCP_4	0.00	-0.19	0.03	0.00	0.71	0.03	0.71	0.00	0.03	0.00	-0.09	-0.09	0.00	-0.09	0.20	-0.09	0.00	-0.09
QCP_5	0.00	-0.19	0.03	0.00	-0.09	0.19	0.71	0.00	-0.09	0.00	-0.09	-0.09	0.00	0.71	0.03	-0.09	0.00	0.03

Symmetry analysis @ QCPs

- Compute the RG flow equations for the conjugate fields:

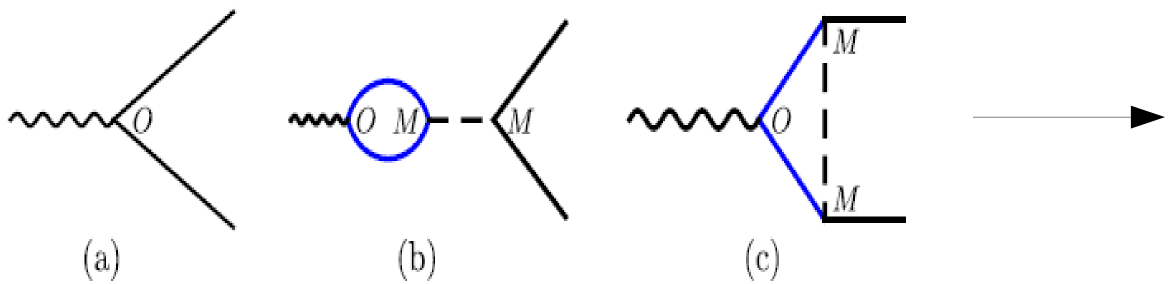

$$\frac{d\ln\Delta_O}{d\ell} - z = \sum_{j=1}^{9} S_O^j\, g_j$$

RHS of the flow equation → scaling dimension of order parameter

@ fixed points when $\{g_i\} \equiv \{g_i^\star\}$

QCP	Scaling dimension of fermion bilinears (in units of ϵ)								
	Pairing								
	A_{1g}(S)	A_{2g}(T)	E_g(S)	A_{1u}(T)	A_{2u}(S)	E_u(T)	$A_{1\mathrm{K}}$(S)	$A_{2\mathrm{K}}$(T)	E_{K}(S)
QCP_1	-0.17	0.00	0.08	-0.17	0.00	0.08	0.00	-0.17	0.08
QCP_2	0.17	0.00	-0.08	0.17	0.00	-0.08	0.00	-0.17	0.08
QCP_3	0.71	0.00	-0.09	-0.09	0.00	0.03	0.00	-0.09	-0.09
QCP_4	0.71	0.00	0.03	-0.09	0.00	-0.09	0.00	-0.09	0.03
QCP_5	-0.09	0.00	0.19	-0.09	0.00	-0.09	0.00	-0.09	-0.09

Emergent symmetry @ QCPs

- QCP$_1$: Quantum anomalous Hall insulator → largest scaling dimension
- QCP$_2$: Charge-density-wave → largest scaling dimension
- QCP$_3$: QSHI & *s*-wave → largest scaling dimension → SO(5) symmetry
  - QCP$_4$: CDW, KVBS & *s*-wave → largest scaling dimension → SO(5) symmetry
    - QCP$_5$: AFM & KVBS → largest scaling dimension → SO(5) symmetry

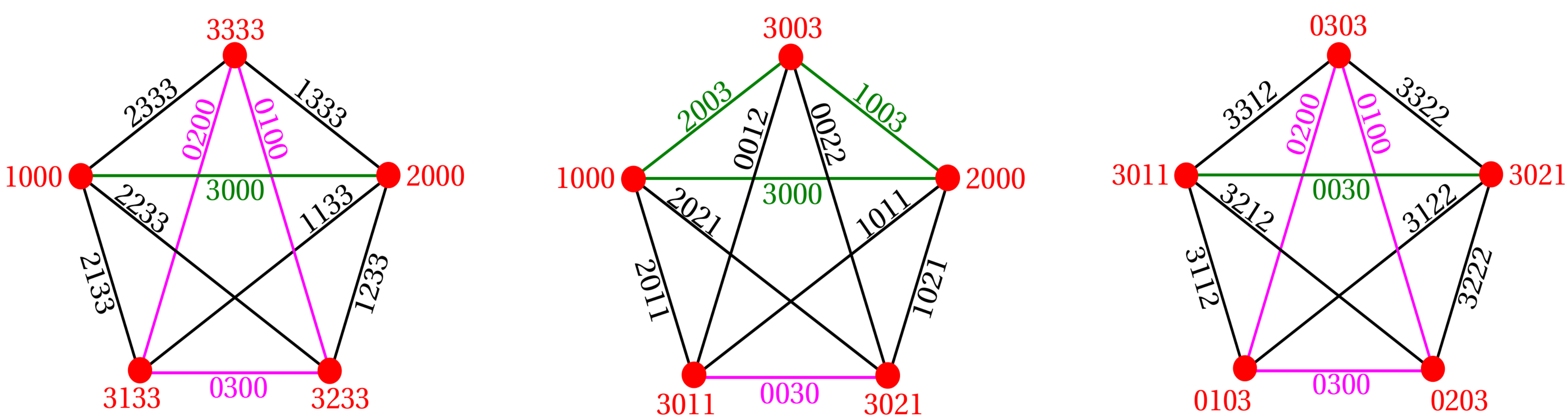

All three SO(5) symmetry → emergent symmetry @ QCPs

- Same results with Lorentz symmetric Wilsonian shell elimination
- Same results with Lorentz symmetry @ microscopic level

How do they manifest on the phase diagram of microscopic models?

Extended Honeycomb Hubbard model

$$H_U = \frac{U}{2} \sum_{R} n_\uparrow(R) n_\downarrow(R),$$

$$H_{V_1} = \frac{V_1}{2} \sum_{\langle A,B \rangle} \sum_{\sigma,\sigma'=\uparrow,\downarrow} n_\sigma(A) n_{\sigma'}(B),$$

$$H_{V_2} = \frac{V_2}{2} \sum_{\langle\langle R,R' \rangle\rangle} \sum_{\sigma,\sigma'=\uparrow,\downarrow} n_\sigma(R) n_{\sigma'}(R')$$

Onsite Hubbard: U
Nearest-neighbor: V_1
Next nearest-neighbor: V_2

Repulsive interaction: $(U,V_1,V_2) > 0$
Attractive interaction: $(U,V_1,V_2) < 0$

- Express the fermionic creation & annihilation operators in terms of Fourier modes around two valley → Initial conditions for microscopic models in terms of the bare values of 9 chosen couplings

- Increase the strength of bare microscopic coupling(s) until at least one coupling diverges: breakdown of nodal Dirac liquid → Onset of ordered state

- Simultaneously at last one conjugate field diverges → Pattern of symmetry breaking

- **Identifying QCP**: At the DSM-Ordered phase boundary running couplings spend a Large amount of RG time in the close vicinity of a QCP before diverging (BSP) or falling back to 0 (DSM) → Pins QCP controlling different segments of the phase boundary

Phase diagram: Kekule Hubbard model

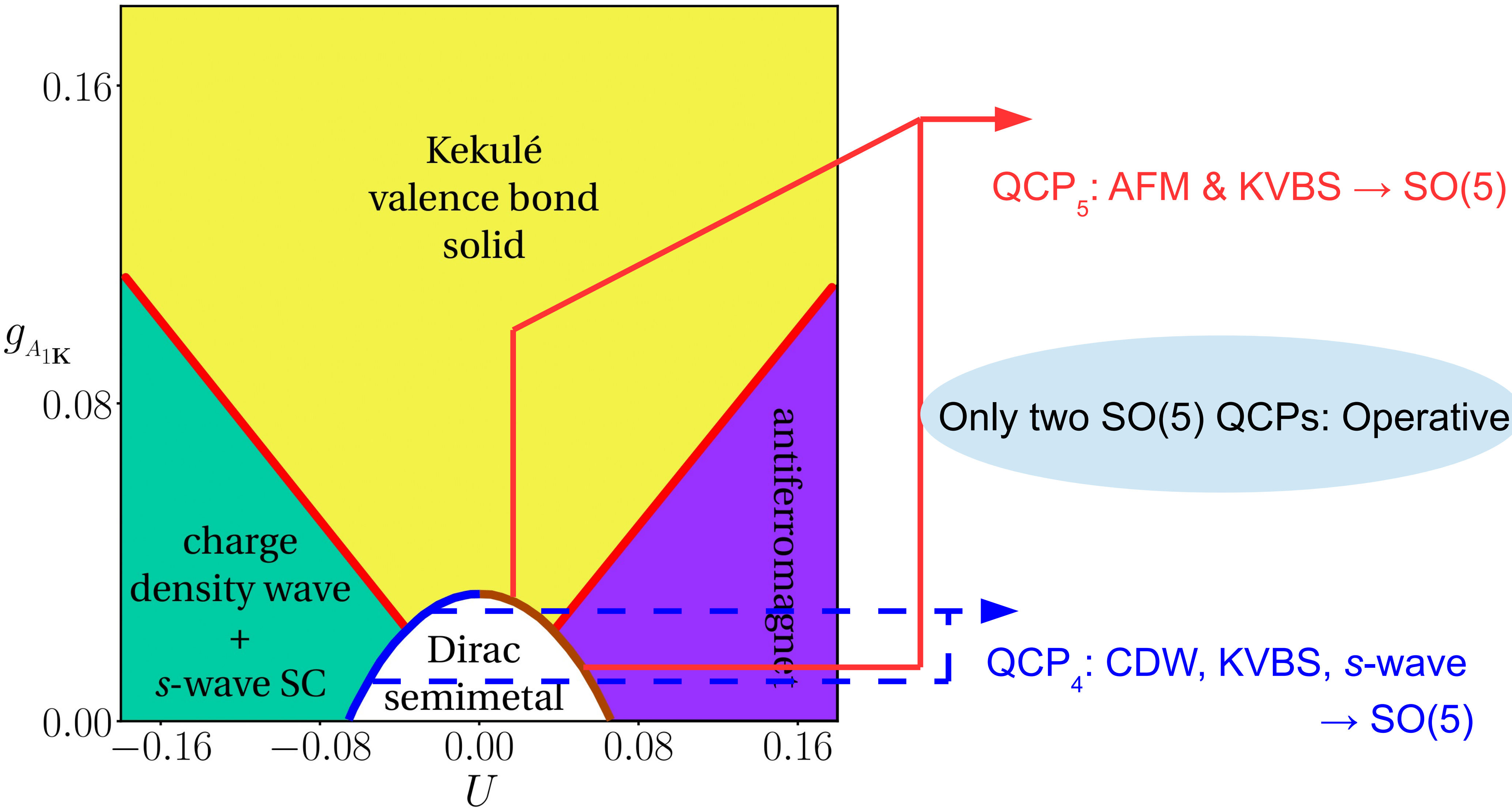

$g_{A1\mathbf{K}}$: Quartic interaction in the KVBS channel

Phase diagram: U-V_1 model

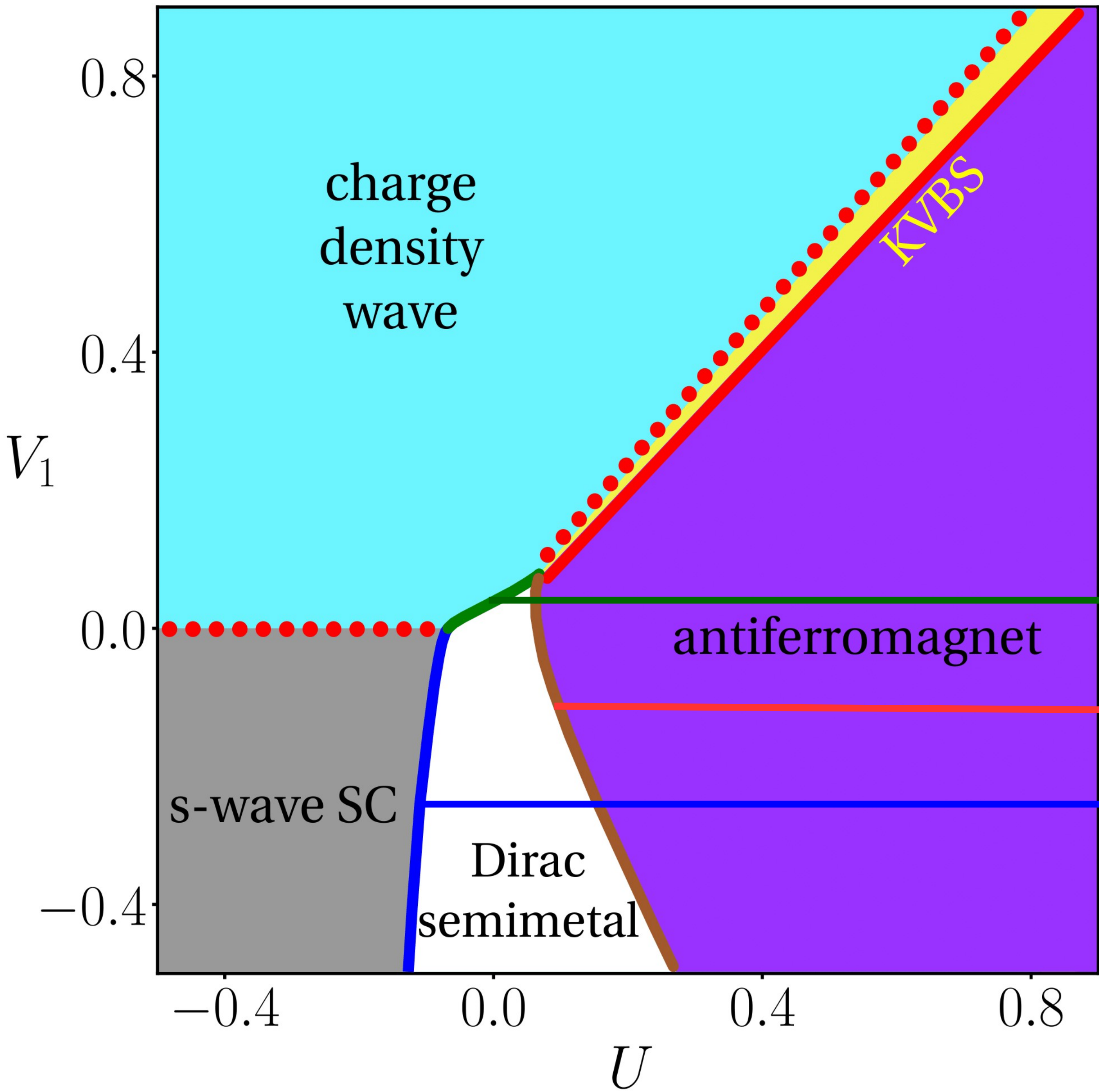

Two SO(5) QCPs & one Z_2 QCP: Operative

QCP_2: Pure CDW

QCP_5: AFM + KVBS → SO(5)

QCP_4: CDW + s-wave + KVBS → SO(5)

Phase diagram: U or V_1-V_2 model

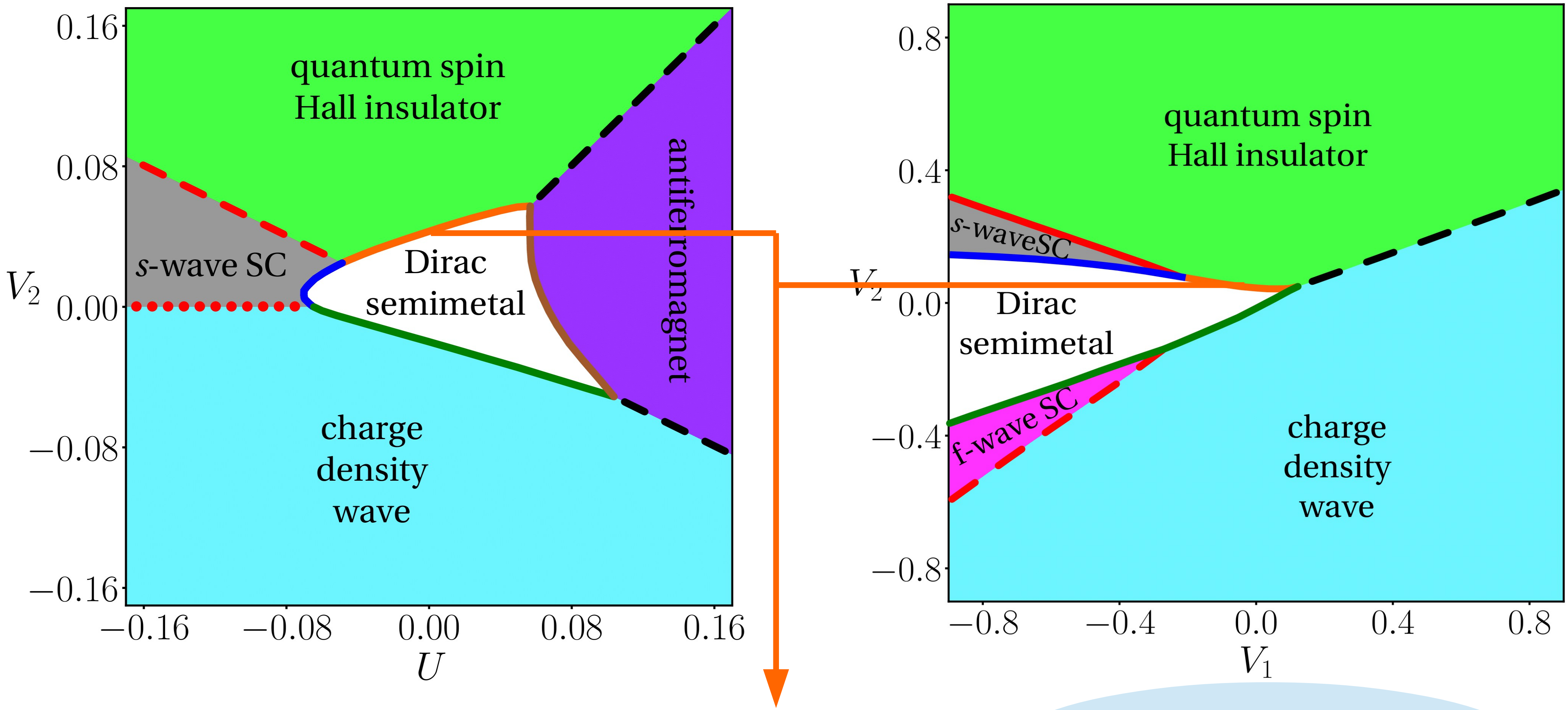

- NNN repulsion → QSHI → Nucleated via QCP_3 :
- Numerical simulations → conflicting outcomes

QSHI + *s*-wave → SO(5)

PRB **89**, 035103 (1014); PRB **92**, 085147 (2015); PRB **92**, 085146 (2015); ...

- Spinless fermions: NNN repulsion → *Quantum Anomalous Hall insulator!*

- Not only internal symmetry between competing orders emerges @ QCPs, but they also control QPTs into either of two phases

- Examples:

  (a) QPTs to AFM & KVBS → controlled by QCP_5 : SO(5) symmetric
  (b) QPTs to *s*-wave & CDW & KVBS → controlled by QCP_4: SO(5) symmetric
  (c) QPTs to QSHI & s-wave → controlled by QCP_3: SO(5) symmetric

- No QCPs with pure AFM, QSHI or *s*-wave order

How about order parameter fluctuation?

Gross-Neveu-Yukawa formalism

$$L_Y = g_1 \sum_{j=1}^{S_1} \Phi_j(x)\Psi^\dagger(x) M_j \Psi(x) + g_2 \sum_{j=S_1+1}^{S} \Phi_j(x)\Psi^\dagger(x) M_j \Psi(x)$$

$$L_b^1 = \sum_{j=1}^{S_1} \left[\frac{1}{2}(\partial_\mu \Phi_j)^2 + m_1^2 \Phi_j^2 + \frac{\lambda_1}{4!}(\Phi_j^2)^2 \right],$$

$$L_b^2 = \sum_{j=S_1+1}^{S} \left[\frac{1}{2}(\partial_\mu \Phi_j)^2 + m_2^2 \Phi_j^2 + \frac{\lambda_2}{4!}(\Phi_j^2)^2 \right],$$

$$L_b^{12} = \frac{\lambda_{12}}{12} \sum_{j=1}^{S_1} \sum_{k=S_1+1}^{S} \Phi_j^2 \, \Phi_k^2.$$

- $O(S_1)$ & $O(S_2)$ symmetry breaking bosonic order parameters: Coupled with gapless Dirac fermions via Yukawa coupling: Composite O(S) order with $S=S_1+S_2$

- AFM: $S_1=3$ & KVBS: $S_2=2 \rightarrow O(S) = O(5)$

  QSHI: $S_1=3$ & *s*-wave: $S_2=2 \rightarrow O(S) = O(5)$

- Perturbative analysis about upper critical three spatial dimension with $\epsilon = 3 - d$

Herbut, Juricic, Vafek PRB **80**, 075432 (2009)

But competing orders need to be introduced from outset!

Emergent symmetry @ Yukawa fixed point

- Pure QCPs with $O(S_1)$ & $O(S_2)$ symmetries (blue and purple dots) are unstable
- Enlarged O(S) symmetry emerges on the critical Hyperplane @ Yukawa fixed point (red dot)
- Controls QPTs from DSM-distinct ordered phases, between two competing ordered phases

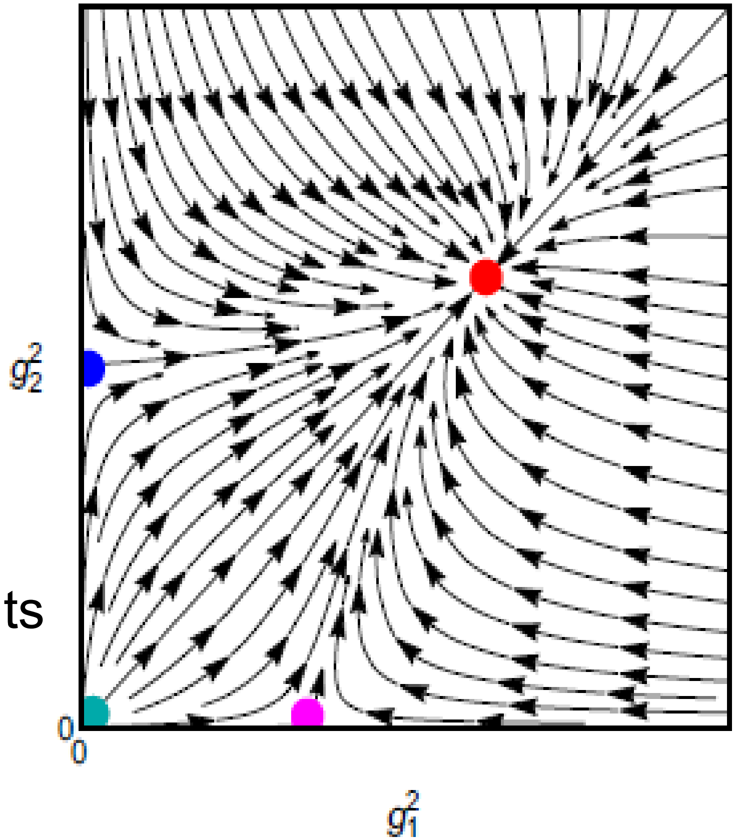

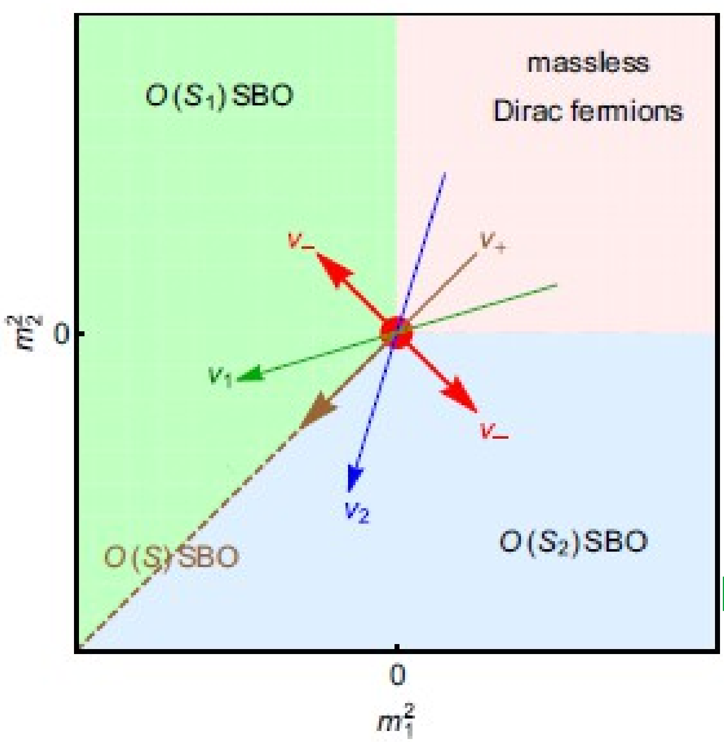

Identical critical exponents

BR PRB **84**, 113404 (2011)
BR, V. Juricic PRB **90**, 041413(R) (2014)
L. Jansen, I. F. Herbut, M. M. Scherer, PRB **97**, 041117(R) (2018)
BR, P. Goswami, V. Juricic, PRB **97**, 205117 (2018)
BR, V. Juricic, PRB **99**, 241103(R) (2019)

Summary

- Correlated nodal semimetal: Ideal platform to demonstrate emergent symmetries @ scale invariant metallic critical points
- Graphene: Massless Dirac fermions on flatland showing emergent SO(5) symmetry among antiferromagnet & valence bond solid, quantum spin-Hall insulator and *s*-wave pairing
- High symmetric QCPs or multi-critical points controls the phase boundaries between DSM and distinct competing ordered phases, as well as direct order-order transition via metallic fixed point
- Emergent symmetry also operative beyond

  (a) Relativistic flatland (3D interacting DSM)

  A. Szabo & BR JHEP **2021**, 4 (2021)

  (b) Beyond relativistic fermions BR & M. Foster, PRX **8**, 011049 (2018)
- Determines nature of competing superconductors @ finite doping

  A. Szabo & BR, PRB **103**, 205135 (2021)